

The BB84 quantum key distribution using conjugate homodyne detection

Bing Qi^{1,2,*}

¹*Quantum Information Science Group, Computational Sciences and Engineering Division,
Oak Ridge National Laboratory, Oak Ridge, TN 37831, USA*

²*Department of Physics and Astronomy, The University of Tennessee, Knoxville, TN 37996, USA*
(Dated: November 19, 2021)

Optical homodyne detection has been widely used in continuous-variable (CV) quantum information processing for measuring field quadrature values. In this paper we explore the possibility of operating a conjugate homodyne detection system in “photon counting” mode to implement discrete-variable (DV) quantum key distribution (QKD) protocols. A conjugate homodyne detection system, which consists of a beam splitter followed by two optical homodyne detectors, can simultaneously measure a pair of conjugate quadratures X and P of the incoming quantum state. In classical electrodynamics, $X^2 + P^2$ is proportional to the energy (the photon number) of the input light. In quantum optics, X and P do not commute and thus the above photon-number measurement is intrinsically noisy. This suggests that a blind application of the standard security proof could result pessimistic QKD performance. We overcome this obstacle by taking advantage of two special features of the proposed detection scheme. First, the fundamental detection noise associated with vacuum fluctuation cannot be manipulated by an external adversary. Second, the ability to reconstruct the photon number statistics at the receiver’s end can place additional constraints on possible attacks from the adversary. As an example, we study the security of the BB84 QKD using conjugate homodyne detection and evaluate its performance through numerical simulations. This study may open the door to a new family of QKD protocols, in complementary to the well-established DV-QKD based on single photon detection and CV-QKD based on coherent detection.

PACS numbers: 03.67.Dd

I. INTRODUCTION

Quantum key distribution (QKD) has drawn great attention for the potential to revolutionize cryptography [1–6]. Presently, the two most well-established families of QKD protocols are discrete-variable (DV) QKD using single photon detection [7, 8] and continuous-variable (CV) QKD using coherent detection (optical homodyne detection) [9–11]. For simplicity, in this paper we refer them as DV-QKD and CV-QKD correspondingly.

On one hand, DV-QKD protocols, such as the celebrated BB84 QKD [7], have been demonstrated over longer distances [12, 13], and enjoy the more mature security proofs especially when system imperfections and finite data size effects are taken into account. On the other hand, CV-QKD protocols, especially the ones based on coherent states [14], have their own advantages, such as implementable using standard telecommunication components and potential high key rate at short distances.

Note that most distinguishing features of CV-QKD can be contributed to optical homodyne detector, which can be implemented with highly efficient photodiodes working at room-temperature. State-of-the-art optical homodyne detector can be operated above tens of GHz with negligible dead-time and a pathway towards fully integrated, on-chip, photonic implementation [15]. In addition, the intrinsic filtering provided by the local oscillator in optical homodyne detection can effectively suppress background noise and enable QKD through conventional dense wavelength division multiplexed fiber networks in the presence of strong classical traffic [16–18] and through daytime free-space channels [19]. A natural question to ask is: can we implement DV-QKD protocols using optical homodyne detection? If possible, it may inherit certain advantages from both worlds. In this paper, we address the above question by studying the BB84 QKD using conjugate optical homodyne detector operated in “photon counting” mode.

A conjugate homodyne detection system, which consists of a beam splitter followed by two optical homodyne detectors, can simultaneously measure a pair of conjugate quadratures X and P of the incoming quantum state by maintaining a 90° phase offset between the two corresponding local oscillators. In classical electrodynamics, $X^2 + P^2$ is proportional to the energy (the photon number) of the input light. In quantum optics, X and P do not commute and thus cannot be determined simultaneously and noiselessly due to Heisenbergs uncertainty principle. This suggests that the above conjugate homodyne detection is intrinsically noisy when operated in photon-

* qib1@ornl.gov

^a This manuscript has been authored in part by UT-Battelle, LLC, under contract DE-AC05-00OR22725 with the US Department of Energy (DOE). The US government retains and the publisher, by accepting the article for publication, acknowledges that the US government retains a nonexclusive, paid-up, irrevocable, worldwide license to publish or reproduce the published form of this manuscript, or allow others to do so, for US government purposes. DOE will provide public access to these results of federally sponsored research in accordance with the DOE Public Access Plan (<http://energy.gov/downloads/doe-public-access-plan>).

counting mode. Intuitively, noisy detectors would result in poor QKD performance if the standard security analysis is employed. To overcome this hurdle, we develop a new security analysis technique exploring two special features of the proposed detection scheme. First, the fundamental detection noise associated with vacuum fluctuation cannot be manipulated by an external adversary (Eve), so it is not necessary to contribute the detector noise to Eve's attack when we estimate a lower bound of Eve's information. This is in line with the trusted detector noise model in CV-QKD [11, 20]. Second, the proposed detection scheme allows the legitimate receiver to reconstruct the photon number statistics of the received light and thus place additional constraints on the possible attacks from Eve. This is similar to the detector decoy QKD, where the photon number statistics at the receiver's end is used to improve QKD performance [21]. As we will show later, by utilizing these two features, a tighter bound on Eve's information and an improved secure key rate can be achieved.

We remark that unlike CV-QKD based on phase-sensitive coherent detection, where sophisticated carrier phase recovery scheme may be required to establish a common phase reference between the transmitter (Alice) and the receiver (Bob) [22, 23], the conjugate homodyne detection scheme adopted in this paper is intrinsically phase insensitive and no phase reference is required.

This paper is organized as follows: in Sec. II, we will review the theory of photon counting using optical homodyne detection [24, 25], and present two possible ways of applying this detection scheme in the BB84 QKD. In Sec. III, we develop a new security analysis method taking into account the special features of the proposed detection scheme, and conduct numerical simulations to evaluate the secure key rates. In Sec. IV, we discuss some practical issues.

II. THE BB84 QKD USING CONJUGATE HOMODYNE DETECTION

A. Conjugate homodyne detection in photon counting mode

Characterizing photon number statistics using optical homodyne detection has been investigated in [24, 25]. Here we follow the discussion in [25]. The basic setup of a conjugate homodyne detection system is shown in Fig. 1. We assume that an unknown quantum state is input from port 1 of a symmetric beam splitter (BS₁ in Fig. 1) and vacuum state is coupled to the other input port. Two optical homodyne detectors are employed to measure the field quadratures of the two output modes. The phase difference between the two corresponding local oscillators is fixed at 90°. In this paper, we assume all the optical homodyne detectors are perfect (noiseless and lossless). We further assume that the unknown input state is in the same mode as the local oscillators.

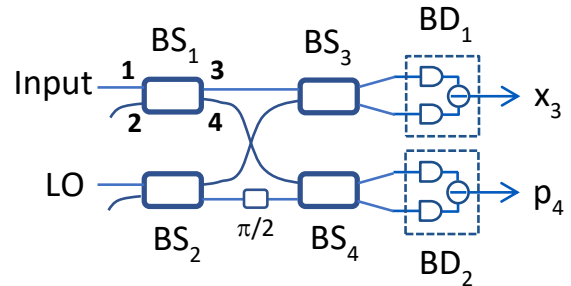


FIG. 1: Conjugate optical homodyne detection. BS₁₋₄: symmetric beam splitter; BD₁₋₂: balanced photodetector; LO: local oscillator.

Given the two local oscillators are sufficiently strong, the outputs of the two homodyne detectors are quadrature components of mode 3 and mode 4 (X_3 and P_4). In [25], a new observable $Z = X_3^2 + P_4^2$ is defined. Given an input state described by the density matrix ρ , the probability density function of Z is given by [25]

$$P_Z(z) = e^{-z} \sum_{n=0}^{\infty} \frac{\rho_{nn}}{n!} z^n, \quad (1)$$

where ρ_{nn} are the diagonal terms of ρ in the Fock basis and $z \geq 0$.

Note that $P_Z(z)$ only depends on the diagonal terms of the density matrix of ρ , as expected from a “phase-insensitive” photon detector. Given a large sample size, the photon number distribution $P_n = \rho_{nn}$ of the input state can be reconstructed from experimentally determined $P_Z(z)$, as shown in [25].

In the case of single-shot measurement, given the input state is a Fock state $|n\rangle$, the likelihood of a measurement output of z can be determined from Eq. (1) [25]

$$P_Z(z|n) = e^{-z} \frac{z^n}{n!}. \quad (2)$$

In the BB84 QKD, threshold single photon detector (SPD), which can discriminate vacuum state from non-vacuum states but cannot resolve photon number, is commonly applied. Two important parameters of a threshold SPD are single-photon detection efficiency and dark count probability. The detection efficiency η_D is defined as the conditional probability that the detector clicks given the input is single-photon state, and the dark count probability v_D is defined as the conditional probability that the detector clicks given the input is vacuum state.

To operate a conjugate homodyne detector in the threshold photon counting mode, we need to map the continuous measurement result z to one of the two possible detection events {click, no-click}. Here, we adopt the same strategy as in [25]: if z is smaller (larger) than

a pre-defined threshold value $\tau \in [0, \infty)$, the detector output is assigned as click (non-click).

Using Eq. (2), the detection efficiency η_D and the dark count probability v_D can be determined by

$$\eta_D = \int_{\tau}^{\infty} P_Z(z|1)dz = e^{-\tau}(\tau + 1) \quad (3)$$

$$v_D = \int_{\tau}^{\infty} P_Z(z|0)dz = e^{-\tau}. \quad (4)$$

In Fig. 2, we present η_D and v_D as functions of the threshold value τ . By choosing an appropriate τ , we could achieve either a high detection efficiency or a low dark count probability, but not both at the same time. For example, when the detection efficiency η_D is about 0.1, the corresponding dark count probability v_D is about 0.02. As a comparison, a state-of-the-art SPD can have a detection efficiency above 0.5 and at the same time, a dark count probability below 10^{-7} per ns [26].

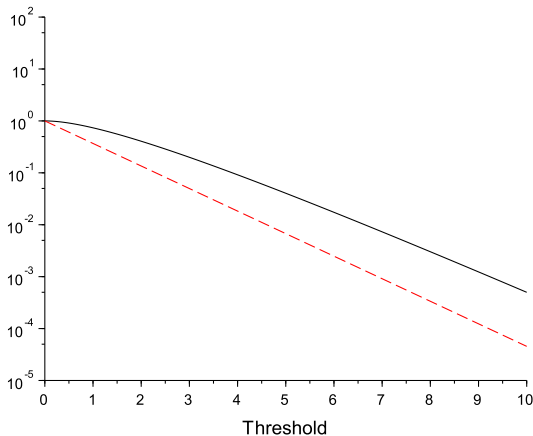


FIG. 2: Simulation results. Detection efficiency η_D (black solid line) and dark count probability v_D (red dashed line) as functions of threshold τ .

At the first sight, the inferior performance of conjugate homodyne detection in photon counting mode seems limit its applications in single-photon based QKD, such as the BB84 protocol. This is probably true if we apply the standard security proof where all the detection noises are contributed to Eve's attack. Such a conservative assumption is necessary when the origins of the noises cannot be identified.

In our case, the measurement uncertainty of the conjugate homodyne detector is due to fundamental quantum noise rather than technical imperfections. So it is not necessary to contribute this noise to Eve's attack when we estimate a lower bound of Eve's information. In next section, we will present an improved security analysis taking into account the special features of the proposed detection scheme. Below we first discuss two different ways

of using a pair of conjugate homodyne detector in the BB84 QKD protocol.

We consider polarization encoding BB84 QKD using perfect single photon source. For each transmission, Alice prepares a single photon pulse with a polarization randomly chosen from $\{H, V, D, A\}$, and sends it to Bob through an insecure quantum channel. Here H (V) refers to horizontal (vertical) polarization state and represents bit 0 (bit 1) in the rectilinear basis, while D (A) represents 45° (135°) polarization state and represents bit 0 (bit 1) in the diagonal basis. At Bob's end, he randomly switches between the two measurement bases and measures the incoming photon using two sets of conjugate homodyne detection systems (D_0 and D_1). To determine a bit value from the outputs of D_0 and D_1 , we consider two possible operation modes: independent detection mode and differential detection mode.

B. Independent detection mode

In this mode, D_0 and D_1 are operated independently as two threshold photon detectors, with detection efficiency and dark count probability given by Eqs. (3) and (4). Due to the symmetry of the protocol, we assume both detectors use the same threshold value τ . There are four possible detection outputs: both detectors click (double-click), only the correct detector clicks, only the wrong detector clicks, and none of them click. The corresponding probabilities are represented by P_D , P_C , P_W , and P_N .

To give an rough estimation of the potential key rate, we calculate the mutual information I_{AB} under the assumption that there is no technical imperfections except the channel loss. Note I_{AB} is not the secure key rate, since we do not consider information could be gained by Eve. Nevertheless, it can serve as a rough upper bound on the secure key rate. We will study lower bounds of secure key rate in next Section.

Given Alice's single photon is prepared in an ideal quantum state corresponding to bit 0, the probability that D_0 clicks is

$$\begin{aligned} P_{D_0}^{(0)} &= \eta_{ch} \int_{\tau}^{\infty} P_Z(z|1)dz + (1 - \eta_{ch}) \int_{\tau}^{\infty} P_Z(z|0)dz \\ &= (\eta_{ch}\tau + 1)e^{-\tau}, \end{aligned} \quad (5)$$

where η_{ch} is the channel transmittance.

The probability that D_1 clicks is simply the dark count probability given by Eq. (4)

$$P_{D_1}^{(0)} = e^{-\tau}. \quad (6)$$

Since the dark count of D_1 is independent of the output of D_0 , the probabilities of the four detection events can be determined from Eqs (5) and (6) as

$$P_N = (1 - P_{D_0}^{(0)})(1 - P_{D_1}^{(0)}) = [1 - (\eta_{ch}\tau + 1)e^{-\tau}][1 - e^{-\tau}] \quad (7)$$

$$P_C = P_{D_0}^{(0)}(1 - P_{D_1}^{(0)}) = (\eta_{ch}\tau + 1)e^{-\tau}(1 - e^{-\tau}) \quad (8)$$

$$P_W = (1 - P_{D_0}^{(0)})P_{D_1}^{(0)} = [1 - (\eta_{ch}\tau + 1)e^{-\tau}]e^{-\tau} \quad (9)$$

$$P_D = P_{D_0}^{(0)}P_{D_1}^{(0)} = (\eta_{ch}\tau + 1)e^{-2\tau}. \quad (10)$$

We assume that Bob post-selects the single photon detection events and throws away no-click and double-click events. The corresponding gain Q and quantum bit error rate (QBER) E are given by

$$Q = P_C + P_W = (\eta_{ch}\tau + 2)e^{-\tau} - 2(\eta_{ch}\tau + 1)e^{-2\tau} \quad (11)$$

$$E = \frac{P_W}{Q} = \frac{e^{-\tau} - (\eta_{ch}\tau + 1)e^{-2\tau}}{Q}. \quad (12)$$

The mutual information between Alice and Bob is given by

$$I_{AB} = Q[1 - H_2(E)], \quad (13)$$

where $H_2(x) = -x\log_2(x) - (1-x)\log_2(1-x)$ is the Shannon entropy.

In this paper we assume the quantum channel is standard optical fiber with an attenuation coefficient of $\gamma = 0.2\text{dB}/\text{km}$. The channel transmittance is given by

$$\eta_{ch} = 10^{-\frac{\gamma L}{10}}, \quad (14)$$

where L is the fiber length in kilometers.

Figure 3 shows the simulation results of I_{AB} as a function of fiber length. In this simulation, the threshold value τ is optimized to maximize I_{AB} .

C. Differential detection mode

In this mode, the continuous outputs z_0 and z_1 of D_0 and D_1 are used jointly to determine the bit value. More specifically, Bob assigns the bit value to 0 (1) if $z_0 > z_1$ ($z_1 > z_0$). Here, we assume that the probability of $z_0 = z_1$ is negligible. Note in this mode, Bob acquires a bit value for every incoming signal, so the gain Q is one.

Given Alice sends bit 0 and the channel transmittance is η_{ch} , with a probability of $1 - \eta_{ch}$, both detectors receive vacuum state. In this case, the error probability (i.e., the probability that $z_0 < z_1$) is simply $1/2$. With a probability of η_{ch} , D_0 receives one photon and D_1 receives vacuum. In this case, the error probability is given by $\int_0^\infty P(z_0|1)\{\int_{z_0}^\infty P_Z(z_1|0)dz_1\}dz_0 = 1/4$, so the average error rate is

$$E = \eta_{ch}\frac{1}{4} + (1 - \eta_{ch})\frac{1}{2} = \frac{1}{2} - \frac{\eta_{ch}}{4}. \quad (15)$$

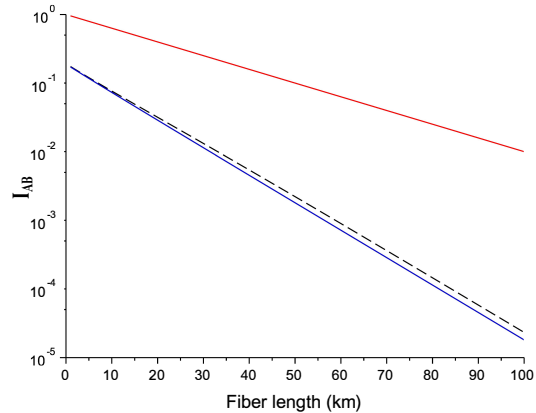


FIG. 3: The mutual information I_{AB} in three cases: perfect SPDs (red solid line), independent detection mode (black dashed line), and differential detection mode (blue solid line).

Again, I_{AB} can be calculated from Eq. (13) and the result is shown in Fig. 3. As a comparison, in Fig. 3, we also present the case when perfect SPDs are employed. In that case $I_{AB} = \eta_{ch}$.

As shown in Fig. 3, I_{AB} determined from the two detection modes are very close to each other. At short distances, both of them are about one order of magnitude below the one achievable with perfect SPDs. Furthermore both of them scale poorer with channel loss. While this may look pessimistic at the first sight, we remark that an optical homodyne detector could be operated at a much higher detection rate than a SPD. So our proposed scheme could still be a viable solution at short distances. We will discuss this issue more in Sec. IV.

III. SECURITY ANALYSIS

A. Standard security analysis

We first calculate secure key rate using the standard security proof of the BB84 implemented with a perfect single photon source. The asymptotic secure key rate is given by [27]

$$R = Q[1 - 2H_2(E)]. \quad (16)$$

Here we assume the efficient BB84 QKD protocol [28] is adopted, that Alice and Bob chose one basis more often than the other (in the asymptotic case the probability of choosing the preferred basis, the rectilinear basis in this paper, approaches to one).

From Eq. (16), to achieve a positive key rate, E has to be less than 11%. This suggests that the differential detection mode cannot work, since the minimum error rate is 25% according to Eq. (15). So we only consider the independent detection mode.

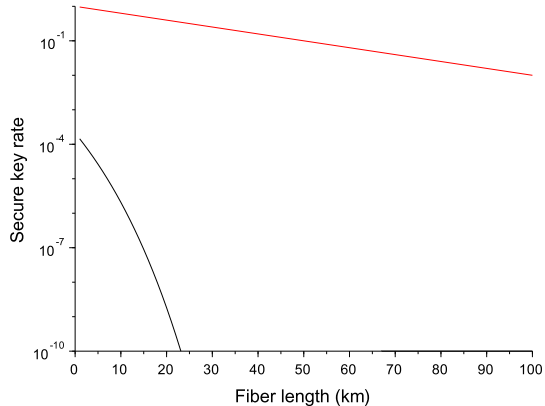


FIG. 4: Secure key rates using the standard security proof [27]. Black line: independent detection mode; red line: perfect SPDs.

Note Eq. (16) is based on the assumption that the quantum state received by Bob is either vacuum or single photon state. However, in practice Eve may intercept Alice's photons and send arbitrary quantum state to Bob, so Eq. (16) cannot be directly applied. Fortunately, a detector squashing model exists in the BB84 QKD [29], which states that as long as the double-click events are kept and assigned with random bit values, Eq. (16) still can be applied. In this case, Q and E can be determined from Eqs. (7)-(10) as

$$Q = 1 - P_N = (\eta_{ch}\tau + 2)e^{-\tau} - (\eta_{ch}\tau + 1)e^{-2\tau} \quad (17)$$

$$E = \frac{P_W + 0.5P_D}{Q} = \frac{e^{-\tau} - 0.5(\eta_{ch}\tau + 1)e^{-2\tau}}{Q}. \quad (18)$$

We conduct numerical simulation and the asymptotic secure key rate is shown in Fig. 4. In this simulation, the threshold value τ is optimized to maximize the secure key rate. As a comparison, we also present the secure key rate for the efficient BB84 using perfect SPDs, which is simply $R = \eta_{ch}$. From Fig. 4, both the secure key rate and the QKD distance of the new detection scheme are very limited. To improve the QKD performance, we develop a new security analysis below.

B. Improved security analysis

We improve the secure key rate by taking advantages of two special features of the proposed detection scheme: the quantum origin of the detection noise and the ability of reconstructing the photon number statistics.

We define the joint probability that Alice transmits m photons and Bob receives n photons as $P_{m,n}$, where m and n are nonnegative integers. The corresponding

yield (conditional detection probability) and QBER are defined as $Y_{m,n}$ and $E_{m,n}$. Since we assume that a perfect single photon source is employed, the only nonzero terms are $P_{1,n}$, $Y_{1,n}$ and $E_{1,n}$. As we have shown in [25], given a large sample size, the photon number statistics of the received quantum state can be fully recovered from the outputs of the detectors. So we assume that the terms $P_{1,n}$ can be fully determined by Bob.

We define the gain of the n -photon state as

$$Q_{1,n} = P_{1,n}Y_{1,n}, \quad (19)$$

where the n -photon state is defined at the receiver's end. Note this is different from the definition in decoy state QKD [30–32], where the n -photon state is commonly defined at Alice's end.

The overall gain Q and the overall QBER E are defined as

$$Q = \sum_{n=0}^{\infty} Q_{1,n} \quad (20)$$

$$E = \frac{\sum_{n=0}^{\infty} Q_{1,n}E_{1,n}}{Q}. \quad (21)$$

To determine the secure key rate, we consider the reverse reconciliation in the classical post processing stage [11], where Bob sends correction information to Alice, who corrects her raw key to have the same values as Bob's. There are three different cases based on the photon number received by Bob:

Case one: Bob receives a vacuum state

In the case, both Alice and Eve have no information about Bob's detection results. No secure key can be generated and there is no need to perform privacy amplification.

Case two: Bob receives one photon

In this case the standard security proof can be applied. Note there is no need to summon to the detector squashing model [29] since Bob receives a qubit.

If Bob could measure the received photon with perfect SPDs, then the QBER in the rectilinear basis can be used to quantify the cost of error correction, while the QBER in the diagonal basis E_X can be used to upper bound Eve's information thus the cost for privacy amplification. However the detection scheme proposed in this paper is intrinsic noisy. Due to the detector noise, both the mutual information between Alice and Bob I_{AB} and Eve's information on Bob's detection results are smaller than the case when perfect SPDs are employed. The I_{AB} term (and the cost for error correction) can be properly quantified by using the actual QBER measured with the noisy detector. As a conservative estimation of Eve's information, here we still use E_X to quantify the cost of privacy amplification. We remark that by further quantifying the decrease of Eve's information due to the detector noise, the secure key rate could be further improved.

Case three: Bob receives more than one photon

The detector responses to multi-photon signals are more complicated and Eve might be able to introduce basis-dependent detection efficiency by sending tailored multi-photon signals. For simplicity, we assume all the multi-photon signals received by Bob are not secure and cannot be used to generate secure key. Again we remark that by developing a more sophisticated detector model, the secure key rate could be further improved in the case when a practical light source (rather than a perfect single photon source) is employed.

Combined the above three cases, the secure key rate is given by

$$R = Q_{1,0} + Q_{1,1}[1 - H_2(E_X)] - QH_2(E), \quad (22)$$

where $Q_{1,0}$ represents the contribution from vacuum state, similar to the case in decoy state QKD [33]. Note that E_X is the expected QBER in the diagonal basis if perfect SPDs are applied. An upper bound of E_X can be obtained from measurable parameters, as we will show below.

Secure key rate: independent detection mode

To apply Eq. (22) to calculate secure key rate, we need to determine five parameters: $Q_{1,0}$, $Q_{1,1}$, Q , E_X and E . Since Q and E can be determined from experimental data directly, below we discuss how to determine the rest.

To determine $Q_{1,0} = P_{1,0}Y_{1,0}$, we need to determine $Y_{1,0}$, the probability that Bob has an effective detection event given he receives a vacuum state. As we noted early, since the photon number statistics at Bob's end is available, we do not need to call for the detector squashing model and can simply throw away all the no-click and double-click events. Using Eq. (2), we have

$$\begin{aligned} Y_{1,0} &= 2 \int_0^\tau P_Z(z_0|0)dz_0 \times \int_\tau^\infty P_Z(z_1|0)dz_1 \\ &= 2(1 - e^{-\tau})e^{-\tau}. \end{aligned} \quad (23)$$

The corresponding QBER is

$$E_{1,0} = 0.5. \quad (24)$$

Similarly, to determine $Q_{1,1}$, we only need to determine $Y_{1,1}$, the probability that Bob has an effective detection given he receives one photon. Under the assumption that the two detector D_0 and D_1 are identical, $Y_{1,1}$ is independent of the polarization state of the received photon, and can be determined by

$$\begin{aligned} Y_{1,1} &= \int_0^\tau P_Z(z_0|1)dz_0 \times \int_\tau^\infty P_Z(z_1|0)dz_1 \\ &+ \int_\tau^\infty P_Z(z_0|1)dz_0 \times \int_0^\tau P_Z(z_1|0)dz_1 \\ &= (\tau + 2)e^{-\tau} - 2(\tau + 1)e^{-2\tau}. \end{aligned} \quad (25)$$

The corresponding QBER is

$$\begin{aligned} E_{1,1} &= (1 - E_X) \frac{\int_0^\tau P_Z(z_0|1)dz_0 \times \int_\tau^\infty P_Z(z_1|0)dz_1}{Y_{1,1}} \\ &+ E_X \frac{\int_0^\tau P_Z(z_0|0)dz_0 \times \int_\tau^\infty P_Z(z_1|1)dz_1}{Y_{1,1}} \\ &= \frac{(E_X\tau + 1)e^{-\tau} - (\tau + 1)e^{-2\tau}}{Y_{1,1}}. \end{aligned} \quad (26)$$

Using Eq. (21), we have

$$\begin{aligned} QE &= Q_{1,0}E_{1,0} + Q_{1,1}E_{1,1} + \sum_{n=2}^{\infty} Q_{1,n}E_{1,n} \\ &\geq Q_{1,0}E_{1,0} + Q_{1,1}E_{1,1}, \end{aligned} \quad (27)$$

which leads to an upper bound of $E_{1,1}$

$$E_{1,1} \leq E_{1,1}^{(u)} = \frac{QE - Q_{1,0}E_{1,0}}{Q_{1,1}}. \quad (28)$$

Once an upper bound of $E_{1,1}$ has been obtained from Eq. (28), an upper bound of E_X can be determined by using Eq. (26). By now, all the parameters needed in Eq. (22) have been derived.

To evaluate the QKD performance, we calculate the secure key rate under normal condition without Eve's attack. Since we assume a perfect single photon source is employed, for a pure loss channel, Bob either receives vacuum state or single-photon state, with the corresponding probabilities $P_{1,0} = 1 - \eta_{ch}$ and $P_{1,1} = \eta_{ch}$. All the other probabilities $P_{1,n} = 0$ for $n \geq 2$. We further assume that the QBER due to polarization misalignment is E_d . Using the above photon number distribution, it is easy to show that $Q_{1,0} = (1 - \eta_{ch})Y_{1,0}$, $Q_{1,1} = \eta_{ch}Y_{1,1}$, $Q = Q_{1,0} + Q_{1,1}$, $E = \frac{0.5Q_{1,0} + Q_{1,1}E_{1,1}}{Q}$, and $E_X = E_d$, where $Y_{1,0}$, $Y_{1,1}$, and $E_{1,1}$ are given in Eqs. (23), (25) and (26).

The simulation results are shown in Fig. 5. In this simulation, the threshold value τ is optimized to maximize the secure key rate. As a comparison, we also present the secure key rate for the BB84 QKD implemented with perfect SPDs. Comparing with the results shown in Fig. 4, we can see that the QKD performance has been greatly improved.

Secure key rate: differential detection mode

The analysis in the differential detection mode is similar to that in the independent detection mode but with a few modifications.

First, in this mode, Bob's detector works in a deterministic fashion, meaning for each incoming signal Bob's detector will output either bit 0 or bit 1. This suggests that $Y_{1,n} = 1$ for any n . So $Q_{1,n} = P_{1,n}$ and $Q = 1$.

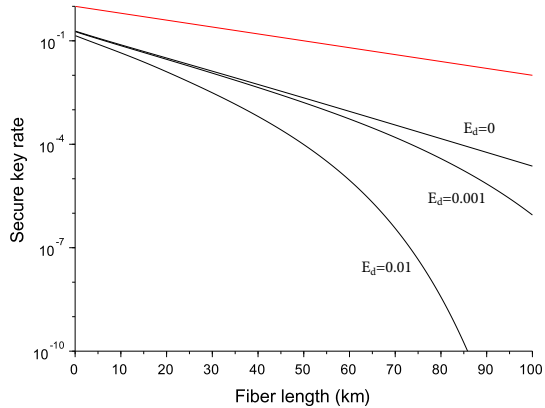


FIG. 5: Secure key rates using the improved security proof (independent detection mode). Black lines: proposed scheme with $E_d = 0, 0.001, 0.01$; red line: perfect SPDs with $E_d = 0$.

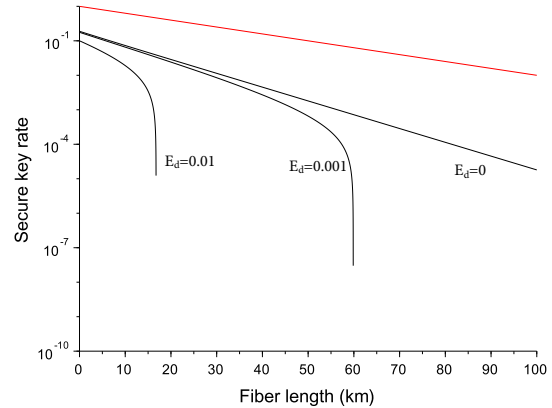


FIG. 6: Secure key rates using the improved security proof (differential detection mode). Black lines: proposed scheme with $E_d = 0, 0.001, 0.01$; red line: perfect SPDs with $E_d = 0$.

Second, $E_{1,0}$ is still 0.5, but $E_{1,1}$ is given by

$$\begin{aligned} E_{1,1} &= (1 - E_X) \int_0^\infty P_Z(z_0|1) \left\{ \int_{z_0}^\infty P_Z(z_1|0) dz_1 \right\} dz_0 \\ &+ E_X \int_0^\infty P_Z(z_0|0) \left\{ \int_{z_0}^\infty P_Z(z_1|1) dz_1 \right\} dz_0 \\ &= \frac{1}{4} + \frac{E_X}{2}. \end{aligned} \quad (29)$$

Again, an upper bound of $E_{1,1}$ can be determined from experimental data by using Eq. (28), then an upper bound of E_X can be obtained by using Eq. (29).

The simulation results are shown in Fig. 6. Comparing with the results shown in Fig. 5, we can see that while both detection modes yield similar key rate in the ideal (noiseless) case, the independent detection mode is more robust against technical imperfection.

IV. DISCUSSION

As shown in Figs. 5 and 6, the performance of the proposed scheme is inferior in compare with the BB84 implemented with conventional SPDs. More specifically, at short distances, the secure key rate of the proposed scheme is about one order of magnitude lower than the conventional approach, and it scales worse with the distance. One may wonder whether the proposed scheme could be a viable solution in practice. Our answer is threefold:

First, in the simulations presented in this paper, both the optical homodyne detectors and SPDs are assumed to be perfect: lossless and noiseless. In practice, the detection efficiency of an optical homodyne detector is typically higher than that of a SPD. This suggests that in

real-life applications, the gap between the two approaches may be smaller than that shown in Figs. 5 and 6.

Second, in this paper the secure key rate is quantified using bits per transmission. In practice, the secure key rate quantified using bits per second is more relevant. Limited by its dead time, the maximum detection rate of a practical SPD is typically below 100MHz. This places a constrain on the achievable secure key rate of the BB84 QKD implemented with this type of detector. On the contrary, an optical homodyne detector shows negligible dead time. This suggests that the proposed scheme could be operated at a much higher rate than the conventional scheme based on SPDs, and may provide a comparable or even higher secure key rate in bits per second over short distances.

Third, as in the case of CV-QKD, the proposed detection scheme can be operated at room temperature, and is highly integratable and robust against broadband background noise. In fact, our scheme is even simpler than the coherent detection scheme used in CV-QKD, since there is no need to establish phase reference between Alice and Bob. To detect Alice's photon efficiently, Bob's local oscillators should be in the same mode as Alice's photon. This requirement is relatively easy to be satisfied and has been routinely demonstrated in the so-called measurement-device-independent QKD [34] with commercial off-the-shelf lasers.

To apply the proposed scheme in practice, there are several challenges to be overcome. First, the present study is based on a perfect single photon source. Unfortunately, such a source is not available in practice. Most of the BB84 QKD implementations are based on phase randomized weak laser sources, which can generate more than one photons occasionally and are susceptible to photon-number splitting attack [35]. Fortunately, in conventional BB84, this problem has been solved by

introducing the so-called decoy state protocols [30–32], where by randomly changing the intensity of the weak laser pulses generated by Alice, the detection statistics of photon number states can be estimated. We expect that the decoy state idea can also be incorporated into the proposed scheme when implemented with a practical laser source. Second, we have ignored the technical imperfections of optical homodyne detectors, including the non-unity detection efficiency and electronic noise. Those imperfections need to be quantified and taken into account in the security analysis. Finally, in this paper we only consider asymptotic cases where all the QKD parameters can be determined precisely. It is important to further investigate the case with finite data size.

In summary, we explore the possibility of operating optical homodyne detectors in photon counting mode to

implement DV-QKD protocols. By developing a new security analysis based on the special features of the detector, we show that reasonable secure key rates could be achieved. This study may open the door to a new family of QKD protocols, in complementary to the well-established DV-QKD based on single photon detection and CV-QKD based on coherent detection.

We acknowledge helpful comments from Nicholas A. Peters and Brian P. Williams. This work was performed at Oak Ridge National Laboratory (ORNL), operated by UT-Battelle for the U.S. Department of Energy (DOE) under Contract No. DE-AC05-00OR22725. The authors acknowledge support from DOE Office of Cybersecurity Energy Security and Emergency Response (CESER) through the Cybersecurity for Energy Delivery Systems (CEDS) program.

-
- [1] N. Gisin, G. Ribordy, W. Tittel, and H. Zbinden, Quantum cryptography, *Rev. Mod. Phys.* **74**, 145 (2002).
- [2] V. Scarani, H. Bechmann-Pasquinucci, N. J. Cerf, M. Dušek, N. Lütkenhaus, and M. Peev, The security of practical quantum key distribution, *Rev. Mod. Phys.* **81**, 1301 (2009).
- [3] H.-K. Lo, M. Curty, and K. Tamaki, Secure quantum key distribution, *Nat. Photon.* **8**, 595 (2014).
- [4] E. Diamanti, H.-K. Lo, B. Qi, and Z. Yuan, Practical challenges in quantum key distribution, *npj Quantum Inf.* **2**, 16025 (2016).
- [5] F. Xu, X. Ma, Q. Zhang, H.-K. Lo, and J.-W. Pan, Secure quantum key distribution with realistic devices, *Rev. Mod. Phys.* **92**, 025002 (2020).
- [6] S. Pirandola, U. L. Andersen, L. Banchi, M. Berta, D. Bunandar, R. Colbeck, D. Englund, T. Gehring, C. Lupo, C. Ottaviani, J. Pereira, M. Razavi, J. S. Shaari, M. Tomamichel, V. C. Usenko, G. Vallone, P. Villoresi, and P. Wallden, Advances in quantum cryptography, arXiv:1906.01645.
- [7] C. H. Bennett and G. Brassard, Quantum cryptography: Public key distribution and coin tossing, in *Proceedings of IEEE International Conference on Computers, Systems and Signal Processing* (IEEE Press, New York, 1984), pp. 175-179.
- [8] A. K. Ekert, Quantum cryptography based on Bell’s theorem, *Phys. Rev. Lett.* **67**, 661 (1991).
- [9] T. C. Ralph, Continuous variable quantum cryptography, *Phys. Rev. A* **61**, 010303(R) (1999).
- [10] M. Hillery, Quantum cryptography with squeezed states, *Phys. Rev. A* **61**, 022309 (2000).
- [11] F. Grosshans, G. V. Assche, J. Wenger, R. Brouri, N. J. Cerf, and Ph. Grangier, Quantum key distribution using gaussian-modulated coherent states, *Nature* **421**, 238 (2003).
- [12] A. Boaron et al., Secure Quantum Key Distribution Over 421 km of Optical Fiber, *Phys. Rev. Lett.* **121**, 190502 (2018).
- [13] S. K. Liao et al., Satellite-to-ground quantum key distribution, *Nature (London)* **549**, 43 (2017).
- [14] E. Diamanti and A. Leverrier, Distributing Secret Keys with Quantum Continuous Variables: Principle, Security and Implementations, *Entropy* **17**, 6072 (2015).
- [15] G. Zhang, J. Y. Haw, H. Cai, F. Xu, S. M. Assad, J. F. Fitzsimons, X. Zhou, Y. Zhang, S. Yu, J. Wu, et al., An integrated silicon photonic chip platform for continuous-variable quantum key distribution, *Nat. Photonics* **13**, 839842 (2019).
- [16] B. Qi, W. Zhu, L. Qian, and H.-K. Lo, Feasibility of Quantum Key Distribution through Dense Wavelength Division Multiplexing Network, *New J. Phys.* **12**, 103042 (2010).
- [17] R. Kumar, H. Qin, and R. Alloume, Coexistence of Continuous Variable QKD with Intense DWDM Classical Channels, *New J. Phys.* **17**, 043027 (2015).
- [18] T. A. Eriksson, T. Hirano, B. J. Puttnam, G. Rademacher, R. S. Luís, M. Fujiwara, R. Namiki, Y. Awaji, M. Takeoka, N. Wada, et al., Wavelength division multiplexing of continuous variable quantum key distribution and 18.3 Tbit/s data channels. *Commun. Phys.* **2**, 9 (2019).
- [19] B. Heim, C. Peuntinger, N. Killoran, I. Khan, C. Wittmann, Ch. Marquardt, and G. Leuchs, Atmospheric Continuous Variable Quantum Communication, *New J. Phys.* **16**, 113018 (2014).
- [20] V. C. Usenko and R. Filip, Trusted noise in continuous-variable quantum key distribution: a threat and a defense, *Entropy* **18**, 20 (2016).
- [21] T. Moroder, M. Curty, and N. Lütkenhaus, Detector decoy quantum key distribution, *New J. Phys.* **11**, 045008 (2009).
- [22] B. Qi, P. Lougovski, R. Pooser, W. Grice, and M. Bobrek, Generating the Local Oscillator “Locally” in Continuous-Variable Quantum Key Distribution Based on Coherent Detection, *Phys. Rev. X* **5**, 041009 (2015).
- [23] D. B. S. Soh, C. Brif, P. J. Coles, N. Lütkenhaus, R. M. Camacho, J. Urayama, and M. Sarovar, Self-Referenced Continuous-Variable Quantum Key Distribution Protocol, *Phys. Rev. X* **5**, 041010 (2015).
- [24] W. Grice and I. A. Walmsley, Homodyne Detection in a Photon Counting Application, *J. Mod. Opt.* **43**, 795 (1996).
- [25] B. Qi, P. Lougovski, and B. P. Williams, Characterizing photon number statistics using conjugate optical homo-

- dyne detection, *Opt. Express* **28**, 2276 (2020).
- [26] R. H. Hadfield, Single-photon detectors for optical quantum information applications, *Nat. Photon.* **3**, 696 (2009).
- [27] P. Shor and J. Preskill, Simple Proof of Security of the BB84 Quantum Key Distribution Protocol, *Phys. Rev. Lett.* **85**, 441 (2000).
- [28] H.-K. Lo, H. F. Chau and M. Ardehali, Efficient quantum key distribution scheme and a proof of its unconditional security, *J. Cryptology* **18**, 133 (2005).
- [29] N. J. Beaudry, T. Moroder, and N. Lütkenhaus, Squashing Models for Optical Measurements in Quantum Communication, *Phys. Rev. Lett.* **101**, 093601 (2008).
- [30] Won-Young Hwang, Quantum Key Distribution with High Loss: Toward Global Secure Communication, *Phys. Rev. Lett.* **91**, 057901 (2003).
- [31] Hoi-Kwong Lo, Xiongfeng Ma, and Kai Chen, Decoy State Quantum Key Distribution, *Phys. Rev. Lett.* **94**, 230504 (2005).
- [32] Xiang-Bin Wang, Beating the Photon-number-splitting Attack in Practical Quantum Cryptography, *Phys. Rev. Lett.* **94**, 230503 (2005).
- [33] H.-K. Lo, Getting something out of nothing, *Quantum Inf. Comput.* **5**, 413 (2005).
- [34] H.-K. Lo, M. Curty, and B. Qi, Measurement-Device Independent Quantum Key Distribution, *Phys. Rev. Lett.* **108**, 130503 (2012).
- [35] G. Brassard, N. Lütkenhaus, T. Mor, and B. C. Sanders, Limitations on Practical Quantum Cryptography, *Phys. Rev. Lett.* **85**, 1330 (2000).